

# The discovery of photospheric nickel in the hot DO white dwarf REJ0503–289<sup>★</sup>

M.A. Barstow<sup>1</sup>, S. Dreizler<sup>2</sup>, J.B. Holberg<sup>3</sup>, D.S. Finley<sup>4</sup>, K. Werner<sup>2</sup>, I. Hubeny<sup>5</sup> and E.M. Sion<sup>6</sup>

<sup>1</sup> *Department of Physics and Astronomy, University of Leicester, University Road, Leicester LE1 7RH, UK*

<sup>2</sup> *Institut für Astronomie und Astrophysik, Universität Tübingen, Waldhäuser Strasse 64, D-72076, Tübingen, Germany*

<sup>3</sup> *Lunar and Planetary Laboratory, University of Arizona, Tucson, AZ 85721, USA*

<sup>4</sup> *Eureka Scientific Inc., 2452 Delmer St., Suite 100 Oakland, CA 94602*

<sup>5</sup> *Laboratory for Astronomy and Solar Physics, NASA/GSFC, Greenbelt, Maryland, MD 20711, USA*

<sup>6</sup> *Department of Astronomy and Astrophysics, Villanova University, Villanova, PA 19085, USA*

31 October 2018

## ABSTRACT

We present the first evidence for the direct detection of nickel in the photosphere of the hot DO white dwarf REJ0503–289. While this element has been seen previously in the atmospheres of hot H-rich white dwarfs, this is one of the first similar discoveries in a He-rich object. Intriguingly, iron, which is observed to be more abundant than Ni in the hot DA stars, is not detected, the upper limit to its abundance ( $\text{Fe}/\text{He} = 10^{-6}$ ) implying a Fe/Ni ratio a factor 10 lower than seen in the H-rich objects ( $\text{Ni}/\text{He} = 10^{-5}$  for REJ0503–289). The abundance of nickel and various other elements heavier than He were determined from GHRS spectra. We used two completely independent sets of NLTE model atmospheres which both provide the same results. This not only reduces the possibility of systematic errors in our analysis but is also an important consistency check for both model atmosphere codes.

We have also developed a more objective method of determining  $T_{\text{eff}}$  and  $\log g$ , from the He lines in the optical spectrum, in the form of a formal fitting of the line profiles to a grid of model spectra, an analogue of the standard procedure utilising the Balmer lines in DA white dwarfs. This gives the assigned uncertainties in  $T_{\text{eff}}$  and  $\log g$  a firm statistical basis and allows us to demonstrate that inclusion of elements heavier than H, He and C in the spectral calculations, exclusively considered in most published optical analyses, yields a systematic downward shift in the measured value of  $T_{\text{eff}}$ .

**Key words:** stars:abundances – stars:atmospheres – stars:white dwarfs – ultraviolet:stars.

## 1 INTRODUCTION

About one quarter of all white dwarfs have helium-rich photospheres and are classified according to the relative strengths of He II and He I lines in their optical spectra. These are determined by the ionization balance of the He plasma, depending on the effective temperature of the star. The DB white dwarfs display only He I absorption lines, and cover the temperature range from  $\approx 11000 - 30000\text{K}$ . Temperatures below  $11000\text{K}$  are too low to excite He I sufficiently to yield observable lines, leading to the featureless

DC white dwarfs. In contrast, the hot DO stars contain He II lines alone, the ionization of helium requiring higher effective temperatures than found in the DB white dwarfs. The upper limit to the DO temperature range, at approximately  $120000\text{K}$ , is associated with the helium, carbon and oxygen-rich PG1159 stars (also denoted as DOZ by Wesemael et al. 1985, WGL), which are the proposed precursors of the DO white dwarfs. The  $45000\text{K}$  lower temperature limit of the DO range is some  $15000\text{K}$  higher than the beginning of the DB sequence, presenting a so-called DO-DB gap between  $30000\text{K}$  and  $45000\text{K}$ , first noted by Liebert et al. (1986). Subsequent surveys of white dwarfs have failed to find examples of He-rich objects within the gap which continues

★ Based on observations made with the Goddard High Resolution Spectrograph on board the Hubble Space Telescope

to present a problem in our understanding of white dwarf evolution.

It is clear, from the existence of the DO-DB gap and the changing ratio of H-rich to He-rich objects, that white dwarf photospheric compositions evolve as the stars cool. A number of physical mechanisms may be operating. For example, the presence of elements heavier than H or He in white dwarf photospheres is the result of radiative forces acting against the downward pull of gravity, preventing these heavy elements sinking out of the atmosphere (e.g. Chayer, Fontaine & Wesemael 1995). A possible explanation of the DO-DB gap is that, following the AGB and PN phases of mass-loss, residual hydrogen mixed in the stellar envelope floats to the surface converting the DO stars into DAs. Later, the onset of convection may mix the hydrogen layer, depending on its thickness, back into the He-rich lower layers, causing the stars to reappear on the DB sequence.

Any understanding of the possible evolutionary processes depends on several important measurements, including the determination of effective temperature, surface gravity and photospheric composition. Several detailed studies have been carried out for DA white dwarfs (e.g. Marsh et al. 1997; Wolff et al. 1998; Holberg et al. 1993, 1994; Werner & Dreizler 1994), but comparatively little work has been carried out on the DO stars. This is partly due to the smaller number of stars available for detailed study, but also arises from the comparative difficulty of establishing a reliable self-consistent temperature determination from the He II lines. The most recent and probably the most detailed study of the DO white dwarf sample has been carried out by Dreizler and Werner (1996). They applied the results of non-LTE model atmosphere calculations to the available optical and UV spectra to determine the atmospheric parameters of 14 stars, confirming the existence of the DO-DB gap. Dreizler and Werner found the mean mass of the white dwarfs in their sample to be  $0.59 \pm 0.08 M_{\odot}$ , very close to the mean masses of the DA and DB samples. A large scatter in heavy element abundances was found, even for stars with similar parameters, and no clear trend along the cooling sequence could be seen.

With such a small sample of DO white dwarfs available for study, each individual object is significant. Discovered as a result of the *ROSAT* WFC all-sky survey in the EUV, the DO white dwarf REJ0503–289 (WD0501–289, MCT0501–2858) is particularly important because of its low interstellar column density (Barstow et al. 1994). As a consequence, it is the only DO white dwarf which can be observed throughout the complete spectral range from optical to X-ray and has been the subject of intense study. However, despite this attention, it has not proved possible to generate a model spectrum that is consistent at all wavelengths. Optical determinations of the effective temperature, from a single ESO NTT spectrum yield a value of  $\approx 70000\text{K}$ , with a log surface gravity of 7.5 (Barstow et al. 1994; Dreizler & Werner 1996). Similar values are obtained from an LTE analysis of the far-UV He II lines in an *ORFEUS* spectrum of the star (Vennes et al. 1998). In contrast, a lower temperature of  $63000\text{K}$  is required to reproduce the flux level of *EUVE* spectrum and simultaneously match the C III and C IV line strengths in the *IUE* high dispersion spectra (Barstow et al. 1996). However, such a low temperature is incompatible with the absence of He I 4471Å and He I 5876Å absorption lines

in the optical spectrum, which provides a lower limit on  $T_{\text{eff}}$  of  $\approx 65000\text{K}$ .

Analyses of *IUE* high dispersion spectra yield measurements of the abundances of C (also obtained from the optical spectrum), N, O and Si and give limits on the presence of Ni and Fe. More recently, phosphorus has also been detected in the REJ0503–289 *ORFEUS* spectrum (Vennes et al. 1998). The presence of heavy elements in the atmosphere of any white dwarf, DO or DA, is known to have a significant effect on the temperature structure of the photosphere and the emergent spectrum. With millions of absorption lines in the EUV wavelength range, the influence of iron and nickel is particularly dramatic. This is illustrated very clearly in the DA stars, where the Fe and Ni opacity produces a steep drop in the observed flux, compared to that expected from a pure H atmosphere (e.g. Dupuis et al. 1995; Lanz et al. 1996; Wolff et al. 1998). In addition, for an H-rich model atmosphere including significant quantities of Fe and Ni, the change in atmospheric structure also alters the predicted Balmer line profiles. Inclusion of these effects, together with a NLTE analysis, has the affect of yielding lower Balmer line effective temperatures compared with those determined from a pure H-model atmosphere. This results in a net downward shift of the temperature scale for the hottest heavy element-rich objects (Barstow Hubeny & Holberg 1998).

Compared to the extensive studies of the effect of Fe and Ni (and other elements) on the atmospheres of DA white dwarfs, as discussed above, little has been done in the case of the DO stars. First, there are few detections of these species in the atmospheres of the DOs (see Dreizler & Werner 1996). Second, it has been more difficult to calculate suitable stellar model atmospheres for comparison with the data. However, it is possible that their inclusion in such computations might eventually solve the problem of the EUV flux. We present an analysis of *HST* spectra of REJ0503–289 obtained with the GHRS, which reveal the presence of Ni in the atmosphere of the star, but yield only upper limits to the abundance of Fe. We analyse a recent optical spectrum of the star, to determine the effective temperature and surface gravity, and evaluate the possible influence of photospheric Ni and trace Fe on the estimated temperature.

## 2 OBSERVATIONS

### 2.1 Optical spectrum

The optical spectrum of REJ0503–289 was obtained by one of us (D.F.) during an observational campaign aimed at the determination of the temperature scale of DA white dwarfs (Finley, Koester & Basri 1997). The spectrum of REJ0503–289 was obtained on 1992 September 22<sup>nd</sup> at the 3 m Shane telescope of the Lick Observatory, using the Kast double spectrograph. The spectrograph was configured to cover the optical wavelength range from 3300Å up to 7500Å in one exposure. A dichroic mirror divides the beam at about 5500Å. The blue spectrum was recorded with a 1200 x 400 Reticon CCD providing a resolution varying from a little over 4Å FWHM at 4000Å to about 6Å FWHM at 5000Å, with an entrance slit width of 2". The red side is recorded separately on a second 1200 x 400 Reticon CCD. Exposure times were set to obtain a peak S/N of  $\approx 100$  in the blue

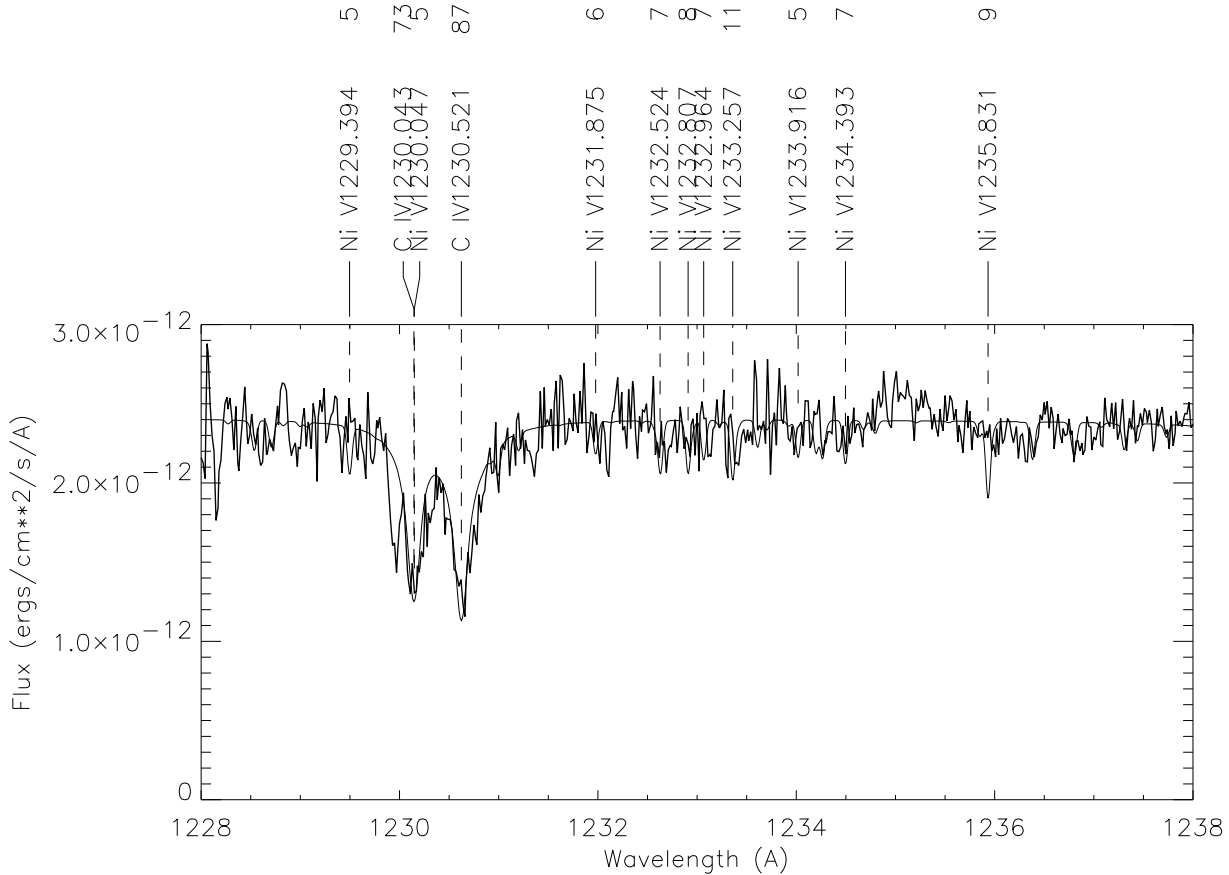


**Figure 1.** a) GHR spectra of REJ0503–289 after coaddition and merging of the individual exposures compared with a theoretical model. All photospheric spectral lines with predicted equivalent width above 5 mÅ are marked, with their identification, laboratory wavelength and predicted equivalent width (mÅ). Note that the annotated equivalent widths are only approximate automated determinations, whereas all values reported elsewhere (in the text and tables) have been accurately measured from the data and synthetic spectra. The C, N, O and Si abundances incorporated in the model were as listed in Table 3. The Fe and Ni abundances chosen from the model grid were both  $10^{-5}$ . The synthetic spectrum has been convolved with a 0.042 Å (fwhm) gaussian function to represent the instrumental response.

spectral region, with the actual S/N ranging from 50 to 110. More details of the instrument set up as well as the data reduction are described by (Finley, Koester & Basri 1997).

## 2.2 GHRs on the Hubble Space Telescope

The *HST* far UV spectra used in this work were obtained from two separate observing programmes carried out during cycle 6 in 1996 and 1997 by two of us (Barstow and Werner), using the Goddard High Resolution Spectrograph (GHRs) before its replacement during the second servicing mission. All spectra utilised the G160M grating, yielding a spectral resolution  $\approx 0.018$  Å rms, the grating angle adjusted to sample different wavelength ranges. The Barstow programme obtained 6 separate exposures covering wavelengths 1233–1271 Å (2 spectra), 1369–1406 Å (3 spectra) and 1619–1655 Å (1 spectrum). The main purpose of the multiple exposures was to monitor any possible variation in absorption line strengths that might be associated with a reported episodic wind (Barstow & Sion 1994). In contrast, the observations of Werner comprised just two single spectra spanning the ranges 1225–1265 Å and 1335–1375 Å. Table 1 summarises all the GHRs observations. Within the observa-

tional errors, there is no evidence for any changes in the profile of any of the N v (1238.8/1242.8 Å), O v (1371.3 Å) and Si iv (1393.8/1402.8) resonance lines. Measurement of the individual equivalent widths (Table 2) also fails to show any of the variability that might be associated with the episodic wind reported by Barstow & Sion (1994).

With no apparent variability and repeated exposure of particular spectral ranges, it is possible to generate a final data set with an overall improvement in signal-to-noise, by merging and coadding the data in an appropriate way. The procedure followed here was to first coadd the results of the initial observations, where the spectral ranges are identical for each exposure, weighting them according to their exposure time. Secondly, the results of this exercise were merged with the later observations, also weighted for exposure time, but only in the regions where the data overlap. The resulting spectra are shown in Fig. 1.

## 2.3 Temporal variability

Although our GHRs spectra of REJ0503–289 show little evidence of temporal variability such variations have been reported from *IUE* data. As previously mentioned,

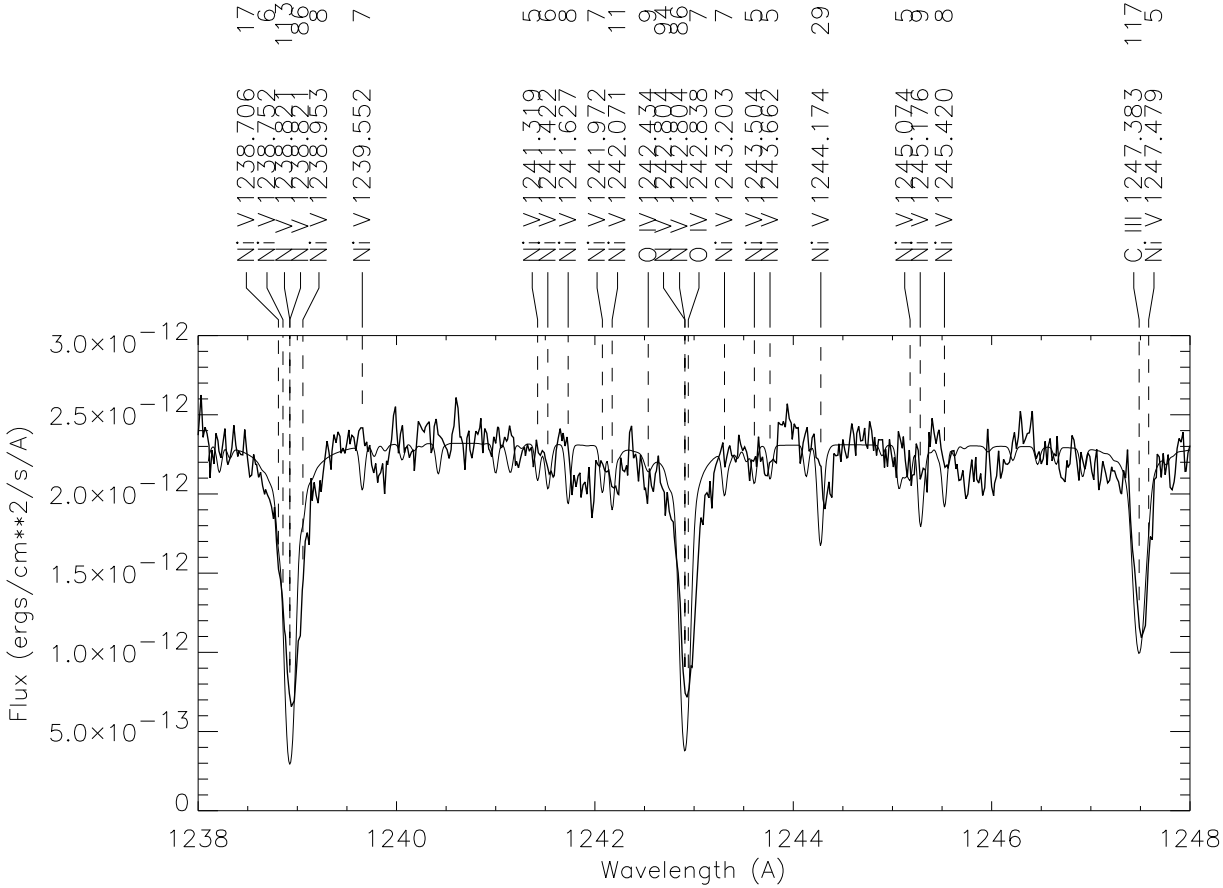


Figure 1 – continued b).

Table 1. Summary of GHRS observations of REJ0503–289

Date	Start time	Wavelength range (Å)	Exposure time (s)	Observer
1996 November 23	07:34:34	1369-1406	653	Barstow
	09:00:58	1233-1271	435	
	09:10:59	1369-1406	544	
	09:22:42	1619-1655	979	
	10:45:44	1369-1406	544	
	10:57:27	1233-1271	435	
1997 January 03	09:22:30	1225-1265	761	Werner
	09:39:22	1335-1375	761	

Barstow & Sion (1994) reported evidence of variations in the C IV, O V and He II features in two SWP echelle spectra of REJ0503–289 obtained 13 months apart. There exist two additional spectra of this star, obtained subsequent to the Barstow & Sion work, which show further evidence of significant variations in the C IV resonance lines (see Holberg, Barstow & Sion 1998). In Fig. 2 we show a comparison of the region of the C IV resonance lines in all four spectra of REJ0503–289, together with the predicted synthetic spectrum computed from a TLUSTY model. As is evident, the two spectra on the right, obtained in Nov. 1994, show much more prominent C IV lines compared with those at the left, obtained in Dec. 1992 and Jan. 1994. In each spectrum a vertical line marks the photospheric velocity of the star. It appears that the most pronounced change is associated with a strengthening of the blue wings of the C IV lines and a

possible development of a blue-shifted component approximately 10 months later in 1994. Similar blue-shifted components are to be found in the majority of the hot He-rich degenerates observed with IUE (Holberg, Barstow & Sion 1998). A discussion of the nature of these blue-shifted features in DO stars is presented in Holberg, Barstow & Sion (1999).

There is additional evidence of temporal variability in the comparison between the equivalent widths as measured in the GHRS data and in the IUE spectra. Holberg, Barstow & Sion (1998) presented results from a coadded version of all four SWP spectra. These authors report equivalent widths for the N V resonance lines which are 30% less than those in Table 6. Such a change in equivalent width is significantly outside the range of mutual uncertainties of the two data

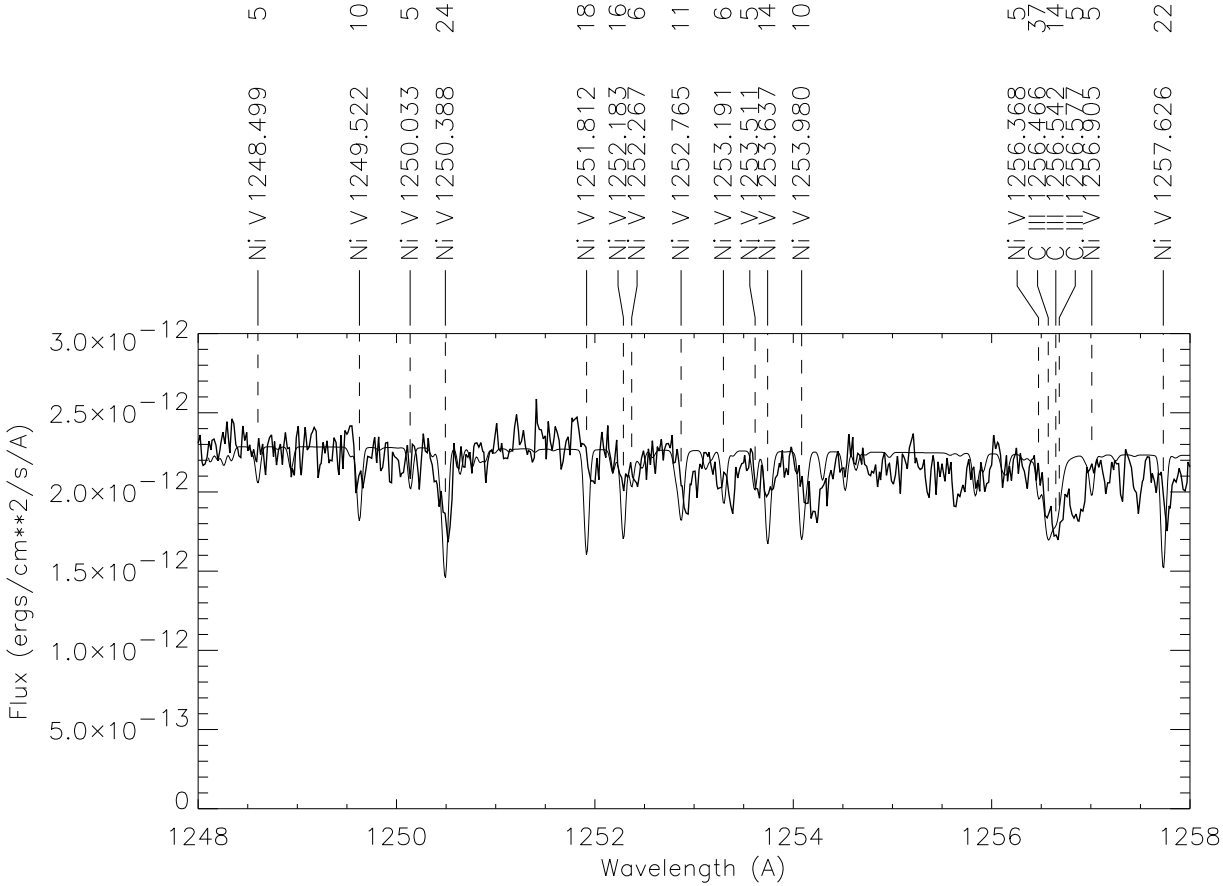


Figure 1 – continued c).

**Table 2.** Equivalent widths (mÅ) of photospheric lines from the multiple exposures. The measurement uncertainties are in brackets.

Date	Start time	N v 1238.3Å	N v 1242.2Å	O v 1371.3Å	Si iv 1393.6Å	Si iv 1402.8Å
1996 November 23	07:34:34			118.6(11.9)	70.9(16.8)	64.8(13.0)
	09:00:58	219.7(17.3)	164.8(15.3)			
	09:10:59			109(13.3)	78.5(14.1)	61.1(15.2)
	10:45:44			128.0(13.3)	78.2(16.0)	58.6(14.3)
	10:57:27	205.6(16.5)	153.1(13.6)			
1997 January 03	09:22:30	220.5(24.1)	175.5(29.1)			
	09:39:22			124.6(21.4)		

sets. The Si IV resonance lines in both data sets, however, remain consistent within mutual errors.

### 3 DATA ANALYSIS

#### 3.1 Non-LTE model atmospheres

We have used theoretical model atmospheres calculated using two independent computer programmes in this study: the TLUSTY code developed by Hubeny (Hubeny 1988; Hubeny & Lanz 1992, 1995) and Werner’s PRO2 suite (Werner 1986, Werner & Dreizler 1999, Dreizler & Werner 1993). Both take account of non-LTE effects in the calculations and include extensive line blanketing.

The TLUSTY models are an extension of work carried out on the atmospheres of hot heavy element-rich DA white dwarfs by Lanz et al. (1996) and Barstow et al. (1998) and have been described extensively in those papers. Briefly,

the models include a total of 26 ions of H, He, C, N, O, Si, Fe and Ni. Radiative data for the light elements have been extracted from TOPBASE, the database for the opacity project (Cunto et al. 1993), except for extended models of carbon atoms. For iron and nickel, all the levels predicted by Kurucz (1988) are included, taking into account the effect of over 9.4 million lines.

To facilitate analysis of both the optical and far UV data sets, an initial grid of models was calculated for determination of effective temperature and surface gravity, spanning a range of  $T_{\text{eff}}$  from 65000K to 80000K (5000K steps) and for  $\log g$  from 7.0 to 8.0 (0.5 dex steps). For computation time reasons, these models only treated the elements H, He and C. It is essential to deal explicitly with carbon because it is the only element, apart from He, visible in the optical spectrum. In addition, the 1548/1550Å resonance lines have a strong influence on the temperature structure of the photospheric models and, as a result, influence the He II line

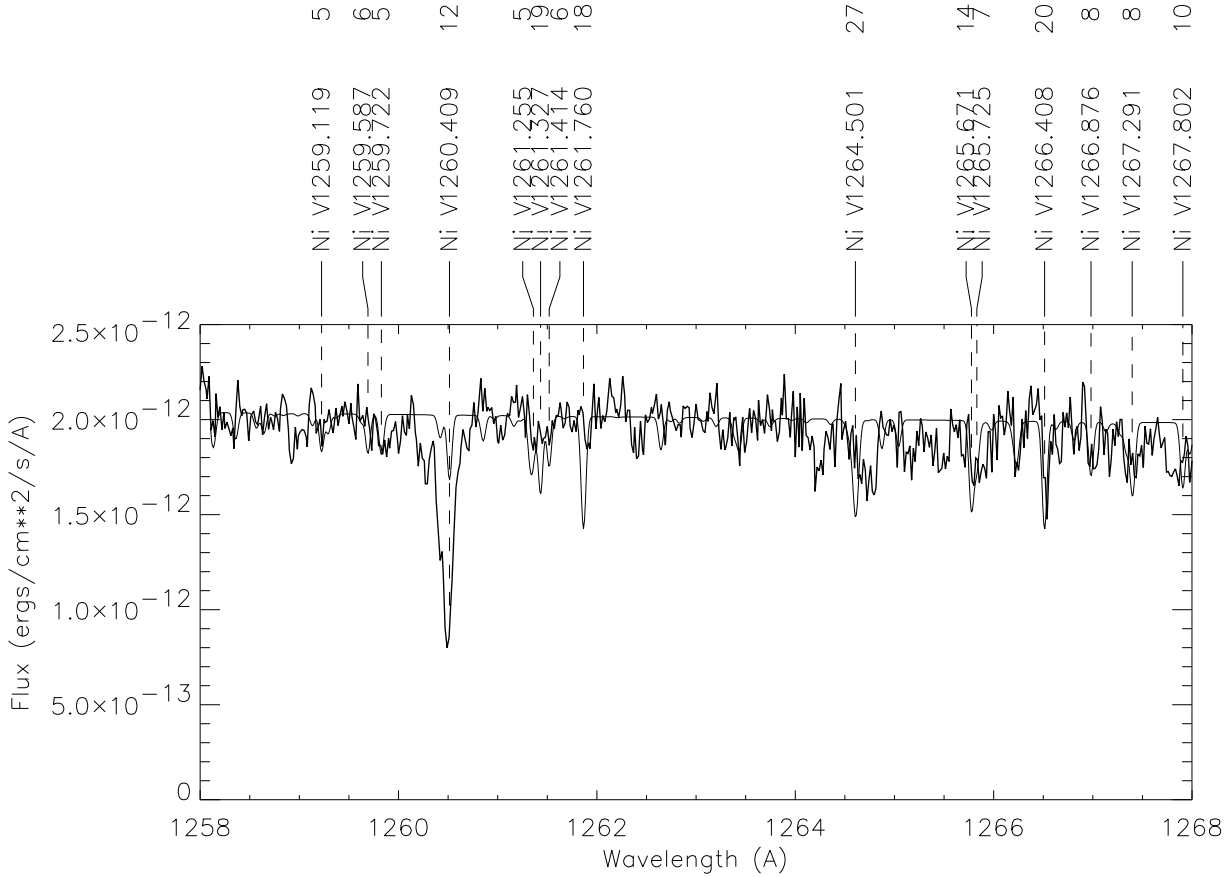


Figure 1 – continued d).

**Table 3.** Element abundances included in TLUSTY model calculations, by number fraction with respect to helium. The Fe and Ni abundance which are in best agreement with the observational data are in bold type. For comparison, the final element abundances as derived with PRO2 models are listed in the third column. Where available the predicted abundances for  $T_{\text{eff}} = 70000\text{K}$  and  $\log g = 7.5$  are listed, from the radiative levitation calculations of Chayer et al. (1995).

Element	Abundance TLUSTY	Abundance PRO2	Abundance rad. lev.
H	$1 \times 10^{-5}$		
He	1.0	1.0	
C	0.005	0.005	0.0002
N	$1.5 \times 10^{-5}$	$1.6 \times 10^{-5}$	$5 \times 10^{-4}$
O	$3 \times 10^{-4}$	$5 \times 10^{-4}$	$2 \times 10^{-4}$
Si	$10^{-5}$	$10^{-5}$	$< 10^{-9}$
Fe	$1 \times 10^{-6} - 3 \times 10^{-5}$	$< 5 \times 10^{-6}$	$2 \times 10^{-4}$
Ni	$1 \times 10^{-5} - 3 \times 10^{-5}$	$1 \times 10^{-5}$	

strengths. The grid was extended to include the heavier elements N, O, Si, Fe and Ni for the single value of  $\log g = 7.5$ , but all values of  $T_{\text{eff}}$ . Table 3 lists the element abundances included in the model grid.

PRO2 is a code for calculating NLTE model atmospheres in radiative and hydrostatic equilibrium using plane-parallel geometry. The PRO2 models are an extension of the work of Dreizler & Heber (1998). In addition to H, He, C, N, and O we included Fe and Ni in the same way as treated by Werner, Dreizler & Wolff (1995). In this set of model

atmospheres we used the previously determined parameters for  $T_{\text{eff}}$  and  $\log g$  (Dreizler & Werner 1996), which took into account the strong influence of H, He and C for the structure of the atmosphere due to the same reasons discussed above.

The physical approximations as well as the atomic input data used in TLUSTY and PRO2 are very similar but the code itself and the numerical techniques as well as the treatment of the atomic data are completely independent. It is, therefore, very interesting to compare the two sets of model atmospheres. Differences allow a reliable estimation of the systematic errors. It is very satisfying from the point of view of the modelers that these are below other uncertainties like the flux calibration of the spectra. This is demonstrated in Table 3 and in Fig. 3, where the 1228Å–1252Å and 1338Å–1375Å regions are compared with synthetic spectra from PRO2 (top) and TLUSTY (bottom). The data are smoothed by a 0.1Å (fwhm) gaussian to reduce the noise in the observed spectrum. It is interesting to note, in Fig. 3, that the line broadening approximation adopted in PRO2 gives slightly better results than that used by TLUSTY /SYNSPEC. Vennes et al. (1998) using IUE and ORFEUS spectra of REJ0503–289, together with LTE models, determined abundances for C, N, and O which on average are over an order of magnitude greater than those determined here. In their study, only Si had a larger abundance, by a factor of 4, than our results.

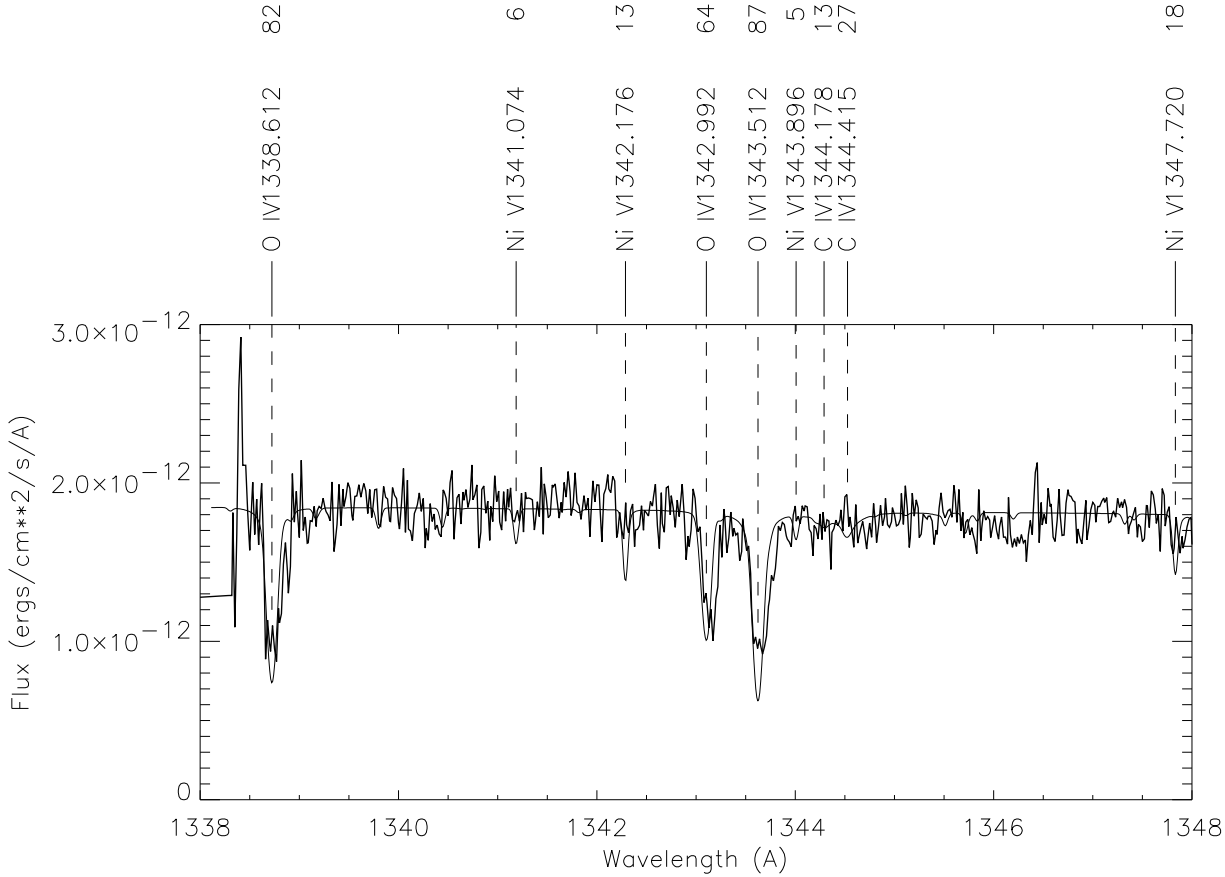


Figure 1 – continued e).

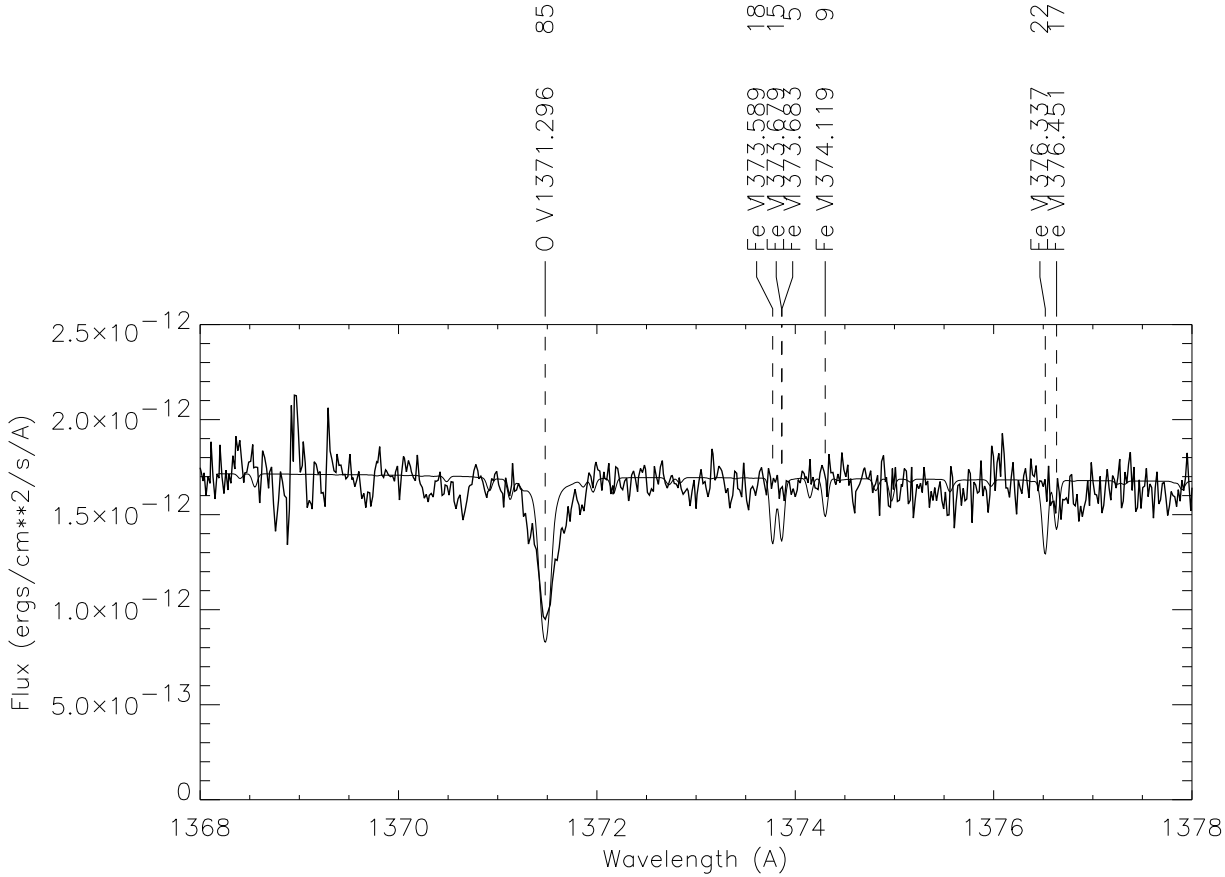
#### 4 AN OPTICAL DETERMINATION OF EFFECTIVE TEMPERATURE AND SURFACE GRAVITY

The technique of using the H Balmer lines to estimate the effective temperatures and surface gravities of the H-rich DA white dwarfs is well-established (e.g. Kidder 1991; Bergeron Saffer & Liebert 1992). These measurements are made by comparing the observed line profiles with the predictions of synthetic stellar spectra, computed from theoretical model atmospheres, searching and interpolating a model grid to find the best match. An objective test, such as a  $\chi^2$  analysis, is used to determine the best-fit solution which also allows formal determination of the measurement uncertainties. While some questions have been raised about the limitations of the technique for the highest temperature DA white dwarfs, with heavy element contaminated atmospheres and weak Balmer lines (Napiwotzki 1992, Napiwotzki & Rauch 1994, Barstow Hubeny & Holberg 1998), it remains the most important and widely used means of determining the DA temperature scale.

In contrast, it has been more difficult to establish a similar standard technique for the DO white dwarfs. This has partly arisen from problems in obtaining good agreement between the models and the data. In particular, it has been difficult to find models that can match all observed He II profiles simultaneously (e.g. see Dreizler & Werner 1996). A particular problem has usually been obtaining a good fit to the  $\lambda 4686$  line. Consequently, in determining  $T_{\text{eff}}$  and  $\log$

g for their sample of DO white dwarfs (the first comprehensive survey), Dreizler & Werner (1996) were forced to rely on a simple visual comparison to select the best-fit model. There is no reason to suppose that the parameters determined for REJ0503–289 and the other DOs studied are seriously in error. However, it is certainly difficult to determine the possible uncertainties in the measurements. Here we develop a more objective approach to obtaining  $T_{\text{eff}}$  and  $\log$  g by fitting the He lines present in the optical spectrum of REJ0503–289 in a manner similar to the technique applied to the DA white dwarf Balmer lines.

Several He II lines are visible in the optical spectrum of REJ0503–289 (Fig. 4), from 4339 Å to 6560 Å. In addition, there are important He I lines at 4471 Å and 5876 Å, not detected in the spectrum, which are very sensitive to effective temperature and, therefore, should be included in any analysis. However, for this spectrum, the 5876 Å line falls in a region of comparatively noisy data, providing a weaker constraint than the 4471 Å feature. Hence, we only consider the latter line in this analysis. For this paper, we have adapted the technique used in our previous work (e.g. Barstow et al. 1998), splitting the spectrum into discrete regions spanned by the absorption lines for comparison with the synthetic spectra. The features included and the wavelength ranges needed to capture the complete lines are listed in Table 4. The complex C IV /He II blend is covered in a single section of data and the He I 4471 Å feature is incorporated with the He II 4542 Å line.

**Figure 1** – *continued f*).**Table 4.** List of He lines used for determination of  $T_{\text{eff}}$  and  $\log g$ , indicating the central wavelength ( $\lambda_c$ ), wavelength range ( $\Delta\lambda$ ), identified lines and their rest wavelengths ( $\lambda_r$ ) considered in the analysis.

$\lambda_c$ (Å)	$\Delta\lambda$ (Å)	Species	$\lambda_r$ (Å)
4339	100	He II	4339
4542	140	He I / He II	4471/4542
4670	100	C IV / He II	4659+4647/4686
4860	100	He II	4860
5400	100	He II	5411
6560	100	He II	6560

We used the programme XSPEC (Shafer et al. 1991) to compare the spectral models with the observational data. XSPEC utilises a robust  $\chi^2$  minimisation routine to find the best match to the data. All the lines included were fit simultaneously and an independent normalisation constant was applied to each, reducing the effect of any wavelength dependent systematic errors in the flux calibration of the spectrum. XSPEC interpolates the synthetic spectra linearly between points in the model grid. Any wavelength or velocity shifts were accounted for by allowing the radial velocity of the lines to vary (taking identical values for each line) during the fit. Once, the best match to the velocity had been obtained, this parameter was fixed, being of no physical interest in this work. The carbon abundance was fixed at a single value of C/He = 0.005 throughout the analysis. Provided the model corresponding to minimum  $\chi^2$  can be

considered to be a ‘good’ fit ( $\chi_{red}^2 < 2$ :  $\chi_{red}^2 = \chi^2/\nu$ , where  $\nu$  is the number of degrees of freedom), the uncertainties in  $T_{\text{eff}}$  and  $\log g$  can be determined by considering the departures in  $\chi^2$  ( $\delta\chi^2$ ) from this minimum. For the two parameters of interest in this analysis (the variables  $T_{\text{eff}}$  and  $\log g$ ), a  $1\sigma$  uncertainty corresponds to  $\delta\chi^2 = 2.3$  (see Press et al. 1992). It should be noted that this only takes account of the statistical uncertainties in the data and does not include any possible systematic effects related to the model spectra or data reduction process.

Fig. 4 and Table 5 show the good agreement achieved between the best fit model and the data. The value of  $\chi_{red}^2$  (1.49) is clearly indicative of a good match between model and data. However, inspection of the fit to the He II 4686 Å line shows that the predicted line strength is weaker than observed, particularly in the line core. If the 4686 Å line is ignored, the agreement between model and data improves, lowering  $\chi_{red}^2$  to 1.38 (see Table 5). There is also an increase in the estimated temperature, from 72660 K to 74990 K, and a slight lowering of the surface gravity (by 0.1 dex).

It has recently been reported by Barstow et al. (1998) that the presence of significant quantities of heavy elements, in particular Fe and Ni, in the atmospheres of DA white dwarfs has a significant effect on the temperature scale. For example, a lower value of the effective temperature is measured from the Balmer line profiles when these elements are included self consistently in the model calculations, in comparison with the results of pure H or H+He models.



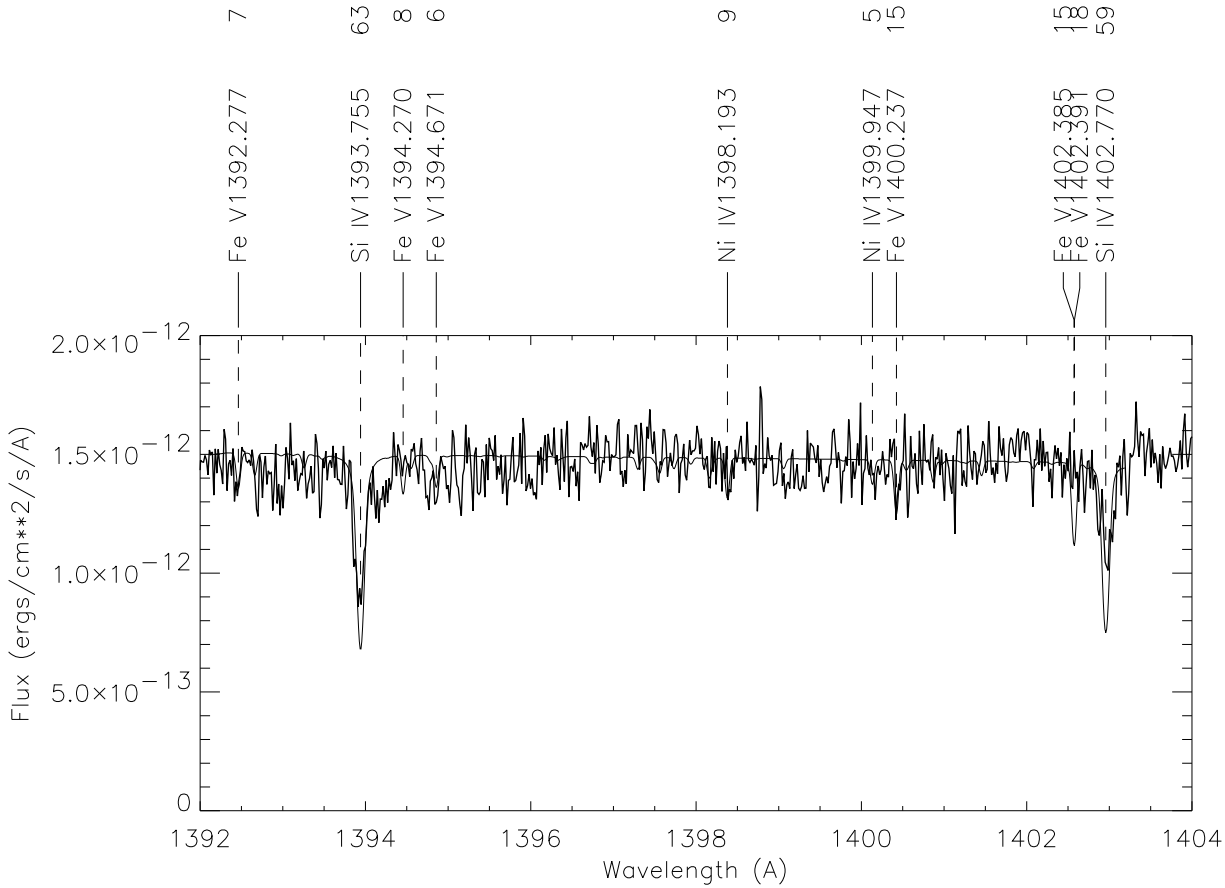


Figure 1 – continued g).

In the analysis of the He-rich star REJ0503–289, discussed here, we included a significant abundance of carbon but no other heavy elements in the theoretical models. However, it is known from earlier work (Barstow & Sion 1994; Barstow et al. 1996) that O, N and Si are definitely present, although at lower abundances (with respect to He) than C, and there were also hints at the possible presence of Fe and Ni.

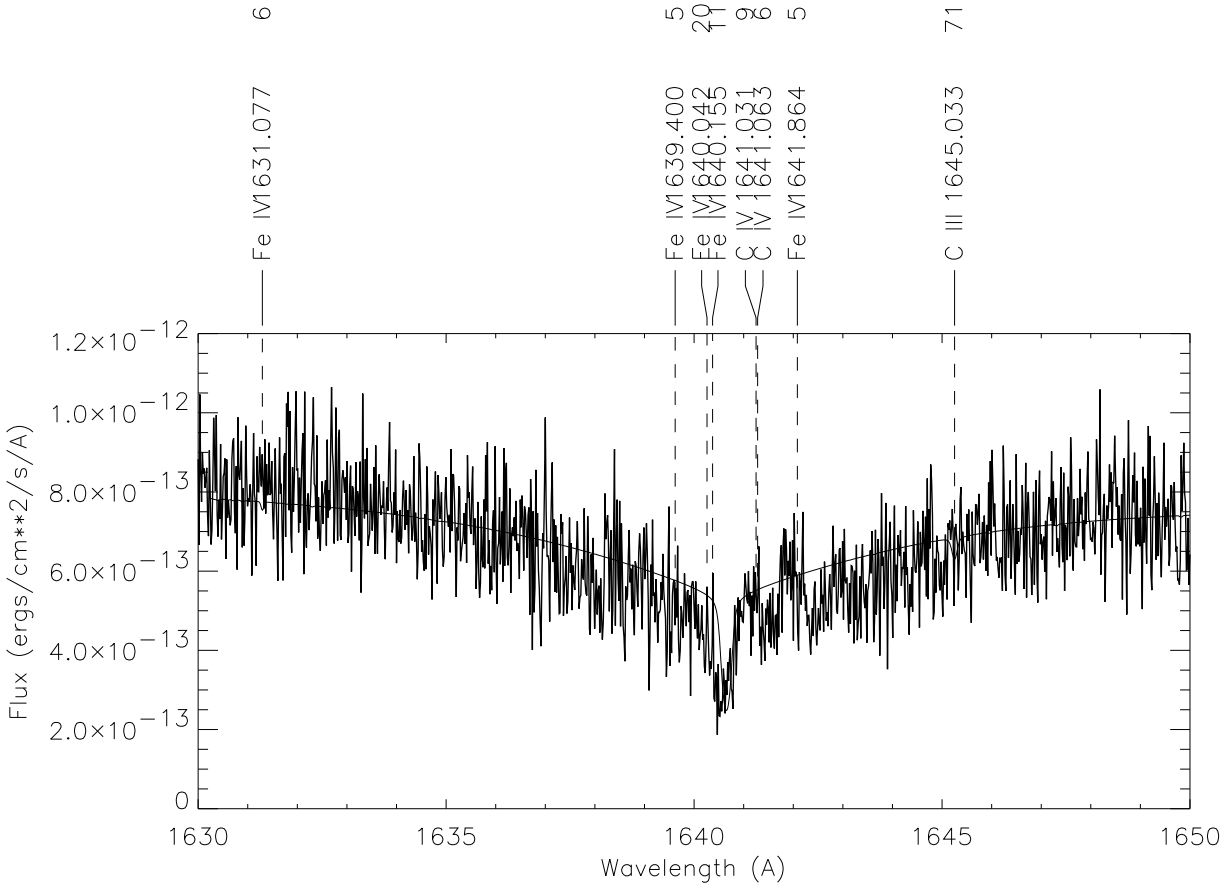
To test the possible effect of these other heavy elements we extended the spectral grid, fixing  $\log g$  at a single value of 7.5 but covering the original 65000K to 80000K temperature range. The nominal heavy element abundances incorporated are listed in Table 3. To assess the possible impact of treating all the heavy elements on the determination of effective temperature, the He lines analysis was repeated using the full heavy element models but with fixed values of the Fe/He and Ni/He abundances ( $10^{-5}$  in both cases). An  $\approx 4\%$  decrease in the effective temperature is seen, but it should be noted that the experimental error bars overlap considerably.

## 5 DETERMINATION OF HEAVY ELEMENT ABUNDANCES FROM THE GHRS DATA

Since the effective temperature and surface gravity of REJ0503–289 are close to 70000K and 7.5 respectively, one of the points of the model atmosphere grid, we adopt these values when applying model calculations to this particular analysis. Fig. 1 shows the merged GHRS spectrum, described in section 2.2, together with a synthetic spectrum

computed for the nominal C, N, O and Si abundances listed in Table 3 and with the Fe and Ni abundances fixed at  $10^{-5}$ . The synthetic spectrum has been convolved with a  $0.042\text{\AA}$  (fwhm) gaussian function to represent the instrumental response. The positions of all lines with a predicted equivalent width greater or equal to  $5\text{m\AA}$  are marked. Several strong lines from highly ionized species of C, N, O and Si are clearly visible, which are most likely to be of photospheric origin. For the most part these have already been identified in the *IUE* echelle spectra of this star (Barstow & Sion 1994; Holberg Barstow and Sion 1998) but we list them here, together with their rest wavelengths, measured wavelengths and measured equivalent widths (Table 6). However, the improved signal-to-noise of the GHRS spectrum, compared to even the coadded *IUE* data allows the detection of several new features, which are included in Table 6. Another important factor may also be the absence of any so-called resseau marks in the GHRS, an important feature of the *IUE* spectra arising from the spatial calibration. Also visible is a single interstellar line of Si II at  $1260.4221\text{\AA}$ .

Apart from these very strongest lines, which are clearly detected, any other possible absorption features are close to the limits of detection imposed by the general signal-to-noise of the data. However, further inspection of Fig. 1 shows a number of coincidences between possible features and predicted Ni V lines. Several of these observed features, at  $1250.4\text{\AA}$ ,  $1257.6\text{\AA}$  (Fig. 1c) and  $1266.4\text{\AA}$  (Fig. 1d), are almost strong enough to constitute detections in their own

**Figure 1** – *continued h*).**Table 5.** Results of the optical spectral analysis carried out using the programme XSPEC, listing the best-fit temperature and surface gravity together with the  $1\sigma$  uncertainties.

Parameter	Fit to all lines	Fit excluding He II 4686Å	Fit to all lines (heavy element models)
$\chi^2$	508.1	398.5	492.9
$\chi^2_{red}$	1.49	1.38	1.45
$T_{eff}$	72660 (66371–75613)	74990 (73150–76630)	70000 (69390–70650)
$\log g$	7.50 (7.35–7.63)	7.41 (7.26–7.53)	7.5 fixed

right. On the basis of these features alone, the evidence for the presence of Ni in the photosphere of REJ0503–289, is not very strong. As a further test we coadded the eight Ni v lines predicted to be the strongest ( $\lambda\lambda$ 1244.23, 1250.41, 1252.80, 1253.25, 1254.09, 1257.66, 1264.62, 1266.40) in velocity space (Fig. 5). This technique has been applied to *IUE* data in the past to detect elements such as Fe and Ni, which do not have any particularly strong resonance transitions but large numbers of comparatively weak features (see e.g. Holberg et al. 1994). The procedure involves shifting the spectra (in this case the GHRs data) into a velocity frame of reference centred on the wavelength of a particular line and then summing and averaging the results for several lines. If apparent weak features are just random fluctuations of the noise the coaddition process will tend to eliminate them whereas, if the features are real, summing the spectra will produce a more significant combined absorption line. The typical experimental uncertainties on the original coadded GHRs spectrum are  $\approx 7 - 10\%$ , whereas the scatter from

data point to data point on the velocity coadded spectrum is around 2%.

Fig. 5 shows the results of the coaddition of the 8 Ni lines. For comparison, the same procedure was carried out for the synthetic spectrum. An absorption feature is clearly detected in both the data and model, at approximately the same strength. This is clear evidence that Ni is present in the photosphere of REJ0503–289 at an abundance of  $\approx 10^{-5}$  with respect to He, although the predicted, coadded line strength is a little stronger than the observation. Interestingly, while there are fewer Fe lines expected to be present in these spectral ranges and their predicted equivalent widths are typically smaller than those of the Ni lines, there are no similar coincidences where significant Fe lines are expected. However, the constraints placed on the Fe abundance by individual lines are not particularly restrictive, only implying an Fe abundance below  $\approx 10^{-5}$  (see Fig. 1f). Again, coaddition of the nine strongest predicted Fe lines ( $\lambda\lambda$ 1361.826, 1373.589, 1373.679, 1376.337, 1376.451, 1378.561, 1387.095, 1387.937, 1402.237) provides a more sensitive indication as

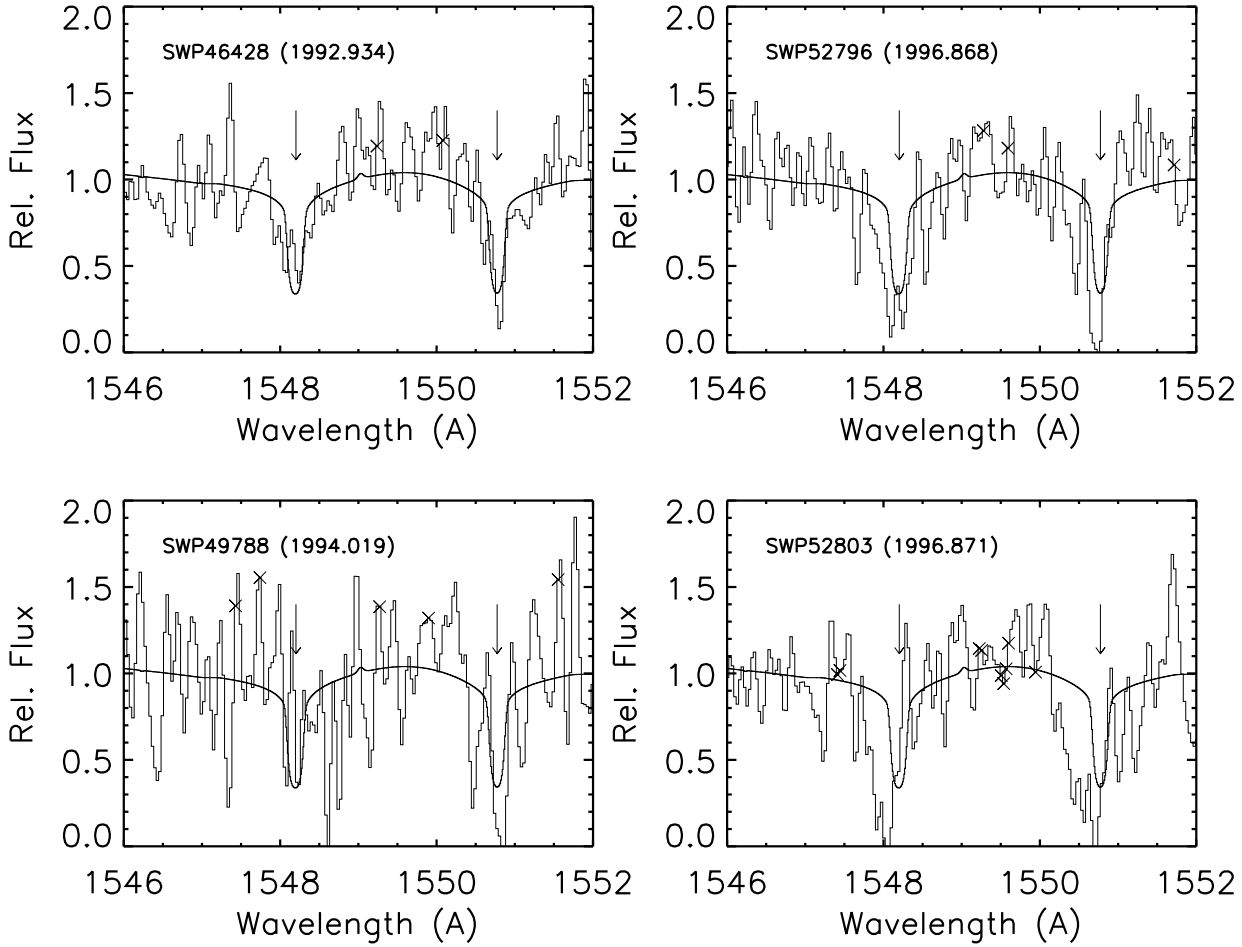


**Figure 2.** A comparison of the region of the C IV resonance lines in the four existing IUE echelle spectra of REJ0503–289 (histogram), illustrating temporal changes in the line profiles. The location of the resonance lines in the photospheric frame are indicated by arrows and synthetic spectrum (smooth curve), calculated using the TLUSTY code is shown for comparison.

to whether or not there is Fe present in the atmosphere (Fig. 6). However, Fe is not detected in this case, as there is no sign of any absorption feature. Comparing the coadded spectrum with models calculated for a range of Fe abundances from  $10^{-6}$  to  $10^{-5}$  (Fig. 6), gives an improved lower limit to the Fe abundance  $\approx 10^{-6}$ .

## 6 DISCUSSION

The availability of GHRs spectra of REJ0503–289, coupled with a new optical spectrum of the star has revealed important information regarding the structure and evolution of this interesting DO white dwarf. We have used the optical spectrum to determine the temperature and surface gravity of the star which is broadly in agreement with earlier determinations from the original ESO optical observation (Barstow et al. 1994; Dreizler & Werner 1996) and the *ORFEUS* far-UV spectrum published by Vennes et al. (1998).

Perhaps the most important part of this particular optical analysis is the more objective determination of the values of  $T_{\text{eff}}$  and  $\log g$ , using a spectral fitting technique, and their respective errors. Whether or not these results might be con-

sidered to be in agreement or disagreement with the results of Vennes et al. (1998) depends somewhat on how we choose to make the measurement, with or without the He II 4686 line and using models with or without the elements heavier than H, He or C. In fact such a comparison is probably not particularly instructive as Vennes et al. used LTE models (compared to our non-LTE calculations) including only H and He. What is important is that we find that the inclusion of heavy elements in the models may have an influence on the outcome of the temperature determination, as it does for the hot DA white dwarfs. Significant abundances of N, O, Si, Fe and Ni (abundances estimated from the GHRs spectra), in addition to the H, He and C treated in the simpler models, lower the value of  $T_{\text{eff}}$  by approximately 2500 K. Nevertheless, a detailed study of any DO star probably needs to be entirely self-consistent, combining temperature/gravity and abundance determinations using spectra from at least visible and UV wavelength ranges. We note that, in this analysis, a higher Fe/He abundance than observed was included in the models used. Therefore, the observed  $T_{\text{eff}}$  change should only be regarded as an upper limit and it must be remembered that systematic errors may be of similar magnitude.

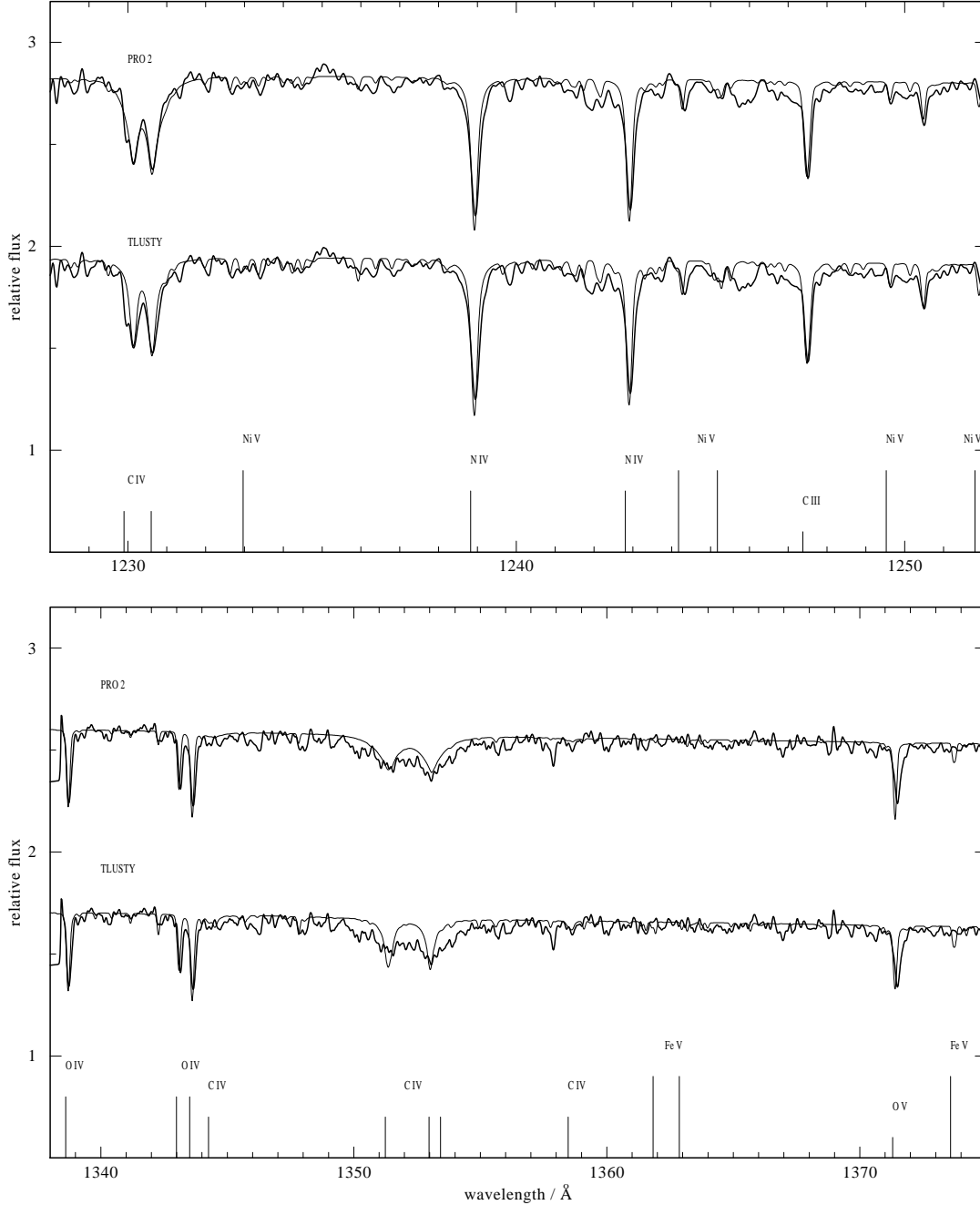


**Figure 3.** Comparison of the PRO2 and TLUSTY model calculations (thin curves). 1228Å to 1252Å (upper panel) and 1338Å to 1375Å (lower panel) regions are shown and matched to the observational data (thick curves), which have been smoothed using a 0.1Å (fwhm) gaussian function to remove some of the noise.

Detections of nitrogen, oxygen and silicon in the far UV spectra have already been reported by other authors (e.g. Barstow et al. 1996; Barstow & Sion 1994; Dreizler & Werner 1996), while carbon is clearly seen in both UV and visible bands. However, while the *IUE* data may have hinted at the presence of Fe and/or Ni (see Barstow et al. 1996), we are able to demonstrate that the star really does contain significant quantities of nickel for the first time, using the GHRs data. This is revealed initially in marginal detections of the strongest individual Ni lines but clearly confirmed when the eight strongest Ni lines are coadded in velocity

space. This is the first detection of Ni in a non-DA white dwarf.

Nickel has also been observed in a number of very hot H-rich DA white dwarfs (e.g. Holberg et al. 1994; Werner & Dreizler 1994) and recently reported for one other hot DO (PG0108+101, Dreizler 2000) but it is always associated with the presence of iron. Furthermore, the measured Fe abundance is typically larger than that of Ni, by factors between 1 and 20. Hence, it is very surprising, given the detection of Ni in REJ0503–289, that we find no evidence at all of any Fe. Not even coadding the regions of

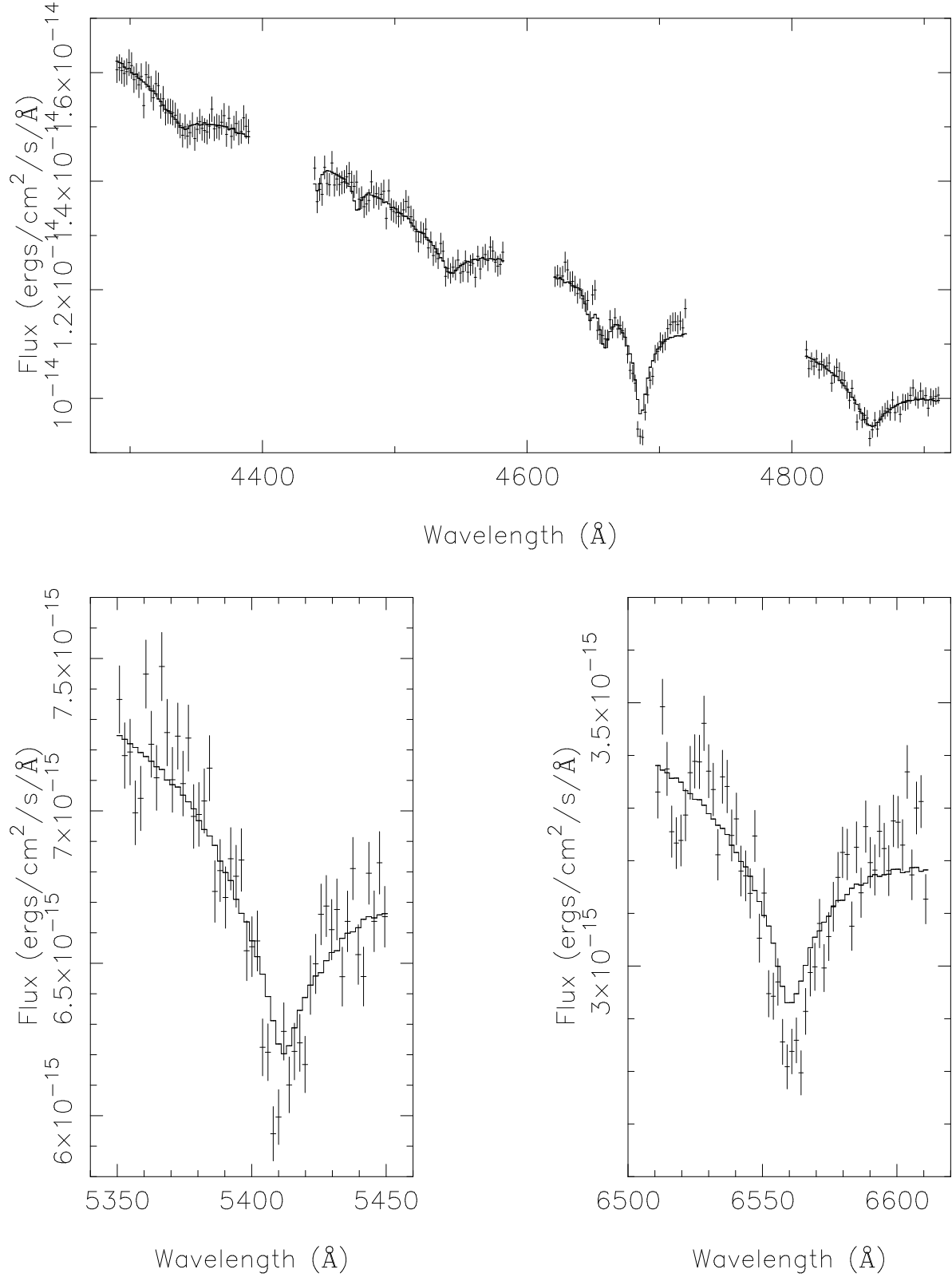


**Figure 4.** Comparison of the observed helium lines (error bars) with the predictions of a synthetic spectrum computed from a model atmosphere including He, H and C. The lines selected for this analysis are (from top to bottom of the figure) listed in Table 5. Top panel – He II 4339, He I / He II 4471/4542, C IV / He II 4659+4647/4686, He II 4860; bottom left panel – He II 5400; bottom right panel – He II 6560.

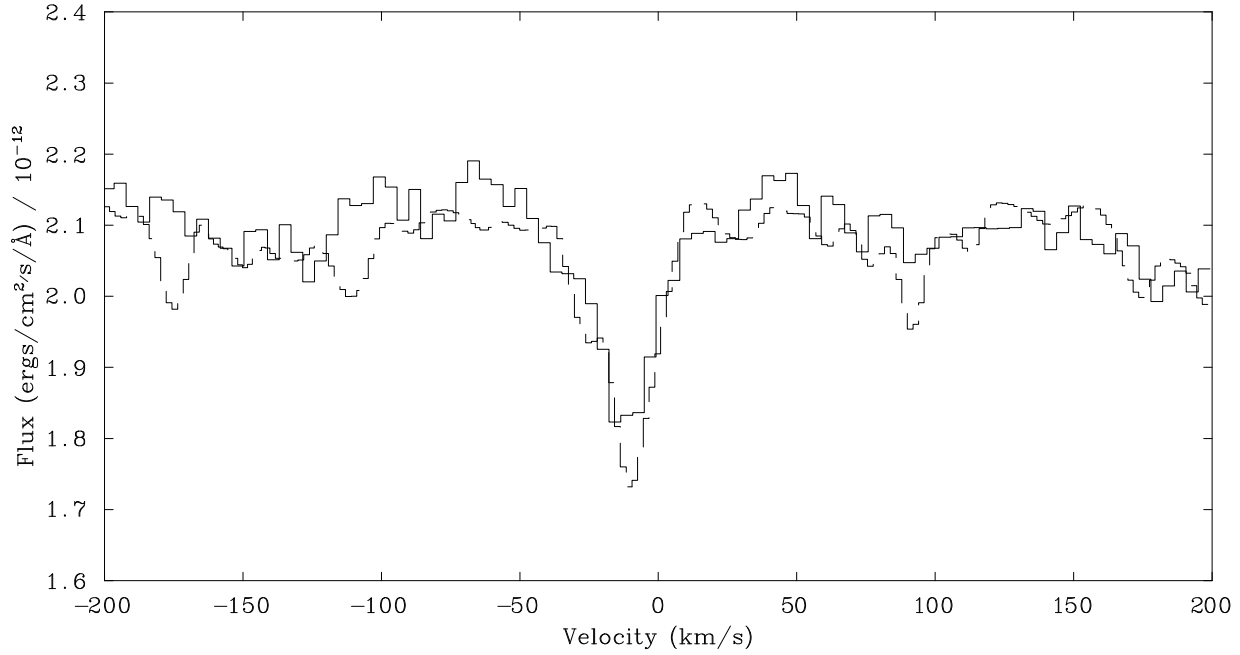


**Figure 5.** The eight Ni V lines predicted to be strongest in the GHRs spectrum coadded in velocity space (solid histogram). A synthetic spectrum, calculated from a model containing a Ni/He ratio of  $10^{-5}$  (dashed histogram) is shown for comparison. All other elemental abundance are as listed in Table 3.

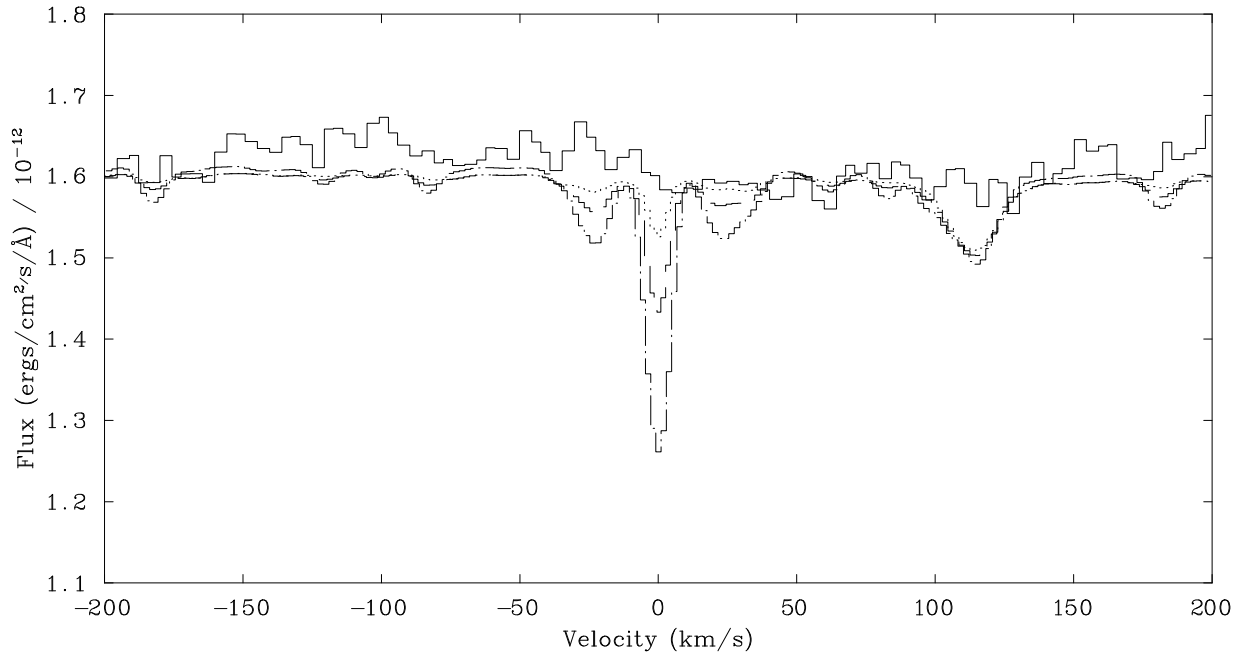


**Figure 6.** The nine Fe V lines predicted to be strongest in the GHRs spectrum coadded in velocity space (solid histogram). Three synthetic spectra, calculated from models containing Fe/He ratios of  $10^{-5}$ ,  $3 \times 10^{-6}$  and  $10^{-6}$  (dot-dashed, dashed and dotted histograms, in order of decreasing line strength) are shown for comparison. All other elemental abundance are as listed in Table 3.

**Table 6.** Absorption lines detected in the GHRS spectrum of REJ0503–289. The figures in brackets are the equivalent widths predicted by a spectral model incorporating the nominal photospheric abundances (see Table 3). No measurements are listed for the C IV lines at 1351.214Å, 1351.286Å and 1352.920Å due to their broad and shallow nature, making the core difficult to locate. Identifications marked (?) are tentative.

Species	Lab. $\lambda$ (Å)	Obs. $\lambda$ (Å)	Error	V (km/s)	Error	EW (mÅ)	Error
Interstellar							
C I (?)	1239.780	1239.822	0.056	10.21	13.53	22.9	10.65
Si II	1260.422	1260.464	0.019	9.96	4.44	112.5	10.98
Photospheric							
C IV	1230.043	1230.181	0.016	33.56	3.87	64.9 (72)	8.6
C IV	1230.521	1230.644	0.019	30.07	4.57	118.4 (87)	11.2
N V	1238.821	1238.936	0.026	27.83	6.36	215.5 (199)	15.2
N V	1242.804	1242.918	0.018	27.60	4.44	155.7 (200)	11.9
C III	1247.383	1247.509	0.013	30.37	3.06	79.0 (117)	8.2
Ni V	1250.388	1250.479	0.019	21.98	4.65	29.1 (26)	7.8
C III	1256.500	1256.627	0.027	30.38	6.40	31.6 (56)	9.0
S VI (?)	1256.802	1256.868	0.031	15.81	7.35	15.9	7.5
O IV	1338.612	1338.764	0.006	33.96	1.43	100.7 (82)	6.3
O IV	1342.992	1343.148	0.010	34.77	2.18	58.6 (67)	6.9
O IV	1343.512	1343.658	0.009	32.58	2.05	90.9 (87)	7.2
C IV	1351.214						
C IV	1351.286						
C IV	1352.920						
O V	1371.296	1371.497	0.020	43.95	4.38	114.6 (84)	11.4
C III	1381.652	1381.851	0.041	43.07	8.85	53.1 (71)	12.5
Si IV	1393.755	1393.932	0.018	38.10	3.76	50.7 (63)	8.5
Si IV	1402.770	1402.964	0.014	41.35	2.88	46.2 (59)	7.5
Mean				33.54	6.09		

the strongest predicted Fe lines in velocity space reveals the slightest hint of an absorption feature. Indeed, this technique allows us to place a tighter upper limit on the abundance of Fe, at  $\approx 10^{-6}$ , than imposed by the individual lines. Thus, the abundance of Ni is greater than the abundance of Fe in REJ0503–289, in the opposite sense to what is observed in the DA white dwarfs, the Fe/Ni ratio being about one order of magnitude lower than found in those stars. Interestingly, the only other DO star with any iron group elements is PG1034+001. KPD0005+5106 was reported to have Fe VII features but GHRS and coadded IUE spectra do not show these features (Werner et al. 1996 and Sion et al. 1997). Dreizler & Werner (1996) find  $\log(\text{Fe}/\text{He}) = -5$  and  $\log(\text{Ni}/\text{He}) < -5$  in PG1034+001. For PG0108+101, Dreizler (2000) gives  $\log(\text{Fe}/\text{He}) = -4.3$  and  $\log(\text{Ni}/\text{He}) = -4.3$ . Thus, the only other DOs with detectable iron and nickel, have Fe/Ni ratios  $> 1$ , like those of the DA stars.

The relative abundances observed in REJ0503–289 are clearly in disagreement with the cosmic abundance ratio of Fe/Ni ( $\approx 18$ ). Unfortunately, the predictions of radiative levitation calculations do not offer much help in explaining the observations. First, while Fe and Ni levitation has been studied in DA white dwarfs, the predicted abundances are much larger than observed, when all possible transitions (from the Kurucz line lists, Kurucz 1992) are included in the calculations (Chayer et al. 1994). Interestingly, better agreement is achieved, for Fe at least, when the subset of lines available in TOPBASE (Cunto et al. 1993) is used and after several physical improvements to the calculations (Chayer et al. 1995). Until recently, no similar calculations were available for Ni. Although much of the radiative levitation work has concentrated on DA white dwarfs, Chayer, Fontaine & Wesemael (1995) did deal with radiative levitation on He-

rich atmospheres, but only considering elements up to and including Fe. The predicted Fe abundance for a star with the temperature and gravity of REJ0503–289 is in excess of  $10^{-4}$ , two orders of magnitude above the level observed by us.

Recently, Dreizler (1999, 2000) has calculated NLTE model atmospheres taking the radiative levitation and gravitational settling self-consistently into account. In agreement with the results of Chayer, Fontaine & Wesemael (1995) the predicted iron abundance is far in excess of the observed one. The observed Fe/Ni ratio, however, can be reproduced qualitatively by these new models, which predict an excess of the nickel abundance over the iron abundance by a factor of three, but it is also clear that the stratified models do not work very well for the DOs, which are best represented by chemically homogeneous calculations.

This clear anomaly mirrors the comparison between predicted and observed abundances for most of the heavy elements (see Table 3). Only the observed abundance of oxygen is close to its predicted value. Consequently, it seems reasonable to conclude that the theoretical calculations are deficient in some way. The Chayer et al. (1995) make very clear statements about what physical effects are considered by their work and what, for various reasonable reasons, they do not deal with. Perhaps the most important limitation is that the current published results for He-rich stars are for static atmospheres whereas there is some evidence for active mass-loss in He-rich objects, including REJ0503–289 (Barstow & Sion 1994). On the other hand, recent studies of DA white dwarf atmospheres show evidence of heavy element stratification (Barstow et al. 1999; Holberg et al. 1999; Dreizler & Wolff 1999). This calls into question the validity of trying to compare ‘abundances’ determined from homoge-

neous models with the radiative levitation predictions where depth dependent elemental abundances are a direct result of the calculations.

## 7 CONCLUSION

We have presented the first direct detection of nickel ( $\text{Ni}/\text{He} = 10^{-5}$ ) in the photosphere of the hot DO white dwarf REJ0503–289 together with a new determination of  $T_{\text{eff}}$  and  $\log g$  utilising an objective spectral fitting technique. Nickel has been seen previously in the atmospheres of hot H-rich white dwarfs, but this is one of the first similar discoveries in a He-rich object, detection of Ni in PG0108+101 having also been recently reported by Dreizler (2000). It is also one of a very small number of detections of Fe group elements in any of the DO white dwarfs. A careful search for the presence of Fe in the star only yields an upper limit of  $\text{Fe}/\text{He} = 10^{-6}$ , implying a Fe/Ni ratio a factor 10 lower than seen in the H-rich white dwarfs. Although there are no published theoretical predictions, from radiative levitation calculations, for the abundance of Ni in He-rich photospheres the observed Fe abundance is some two orders of magnitude below that expected. An explanation of the observed heavy element abundances in this star clearly requires new studies of the various competing effects that determine photospheric abundance, including radiative levitation and possible mass loss via winds. In addition, model atmosphere calculations need to consider the possible effect of depth-dependent heavy element abundances. Some work of this nature has already been undertaken for DA white dwarfs but is only just beginning for He-rich objects. This work appears to be necessary to explain the continued problem of the inconsistency between the results of the far-UV analyses and the EUV spectrum, which cannot be matched by a model incorporating the abundances measured here at the optically determined temperature, the predicted EUV flux level exceeding that observed by a factor 2–3. However, the early indication of studies using self-consistent stratified models is that they do not match the observations very well.

## ACKNOWLEDGEMENTS

The work of MAB was supported by PPARC, UK, through an Advanced Fellowship. JBH and EMS wish to acknowledge support for this work from NASA grant NAG5-3472 and through grant GO6628 from the Space Telescope Science Institute, which is operated by the Association of Universities for Research in Astronomy, incorporated under NASA contract NAS5-26555. *HST* data analysis in Tübingen is supported by the DLR under grants 50 OR 96029 and 50 OR 97055. Data analysis and interpretation were performed using NOAO IRAF, NASA HEASARC and Starlink software. We would like to thank the support scientists at the Space Telescope Science Institute for their help in producing successful observations of REJ0503–289.

## REFERENCES

Barstow M.A., Holberg J.B., Werner K., Buckley D.A.H., Stobie R.S., 1994, *MNRAS*, 267, 653

Barstow M.A., Hubeny I., Holberg J.B., 1998, *MNRAS*, 299, 520  
 Barstow M.A., Hubeny I., Lanz T., Holberg J.B., Sion E.M., 1996, in *Astrophysics in the Extreme Ultraviolet*, eds. S. Bowyer and R.F. Malina, Kluwer, 203  
 Barstow M.A., Sion E.M., 1994, *MNRAS*, 271, L52  
 Barstow M.A., Hubeny I., Holberg J.B., 1999, *MNRAS*, in press  
 Bergeron P., Saffer R.A., Liebert J., 1992, *ApJ*, 394, 228  
 Chayer P., LeBlanc F., Fontaine G., Wesemael F., Michaud G., Vennes S., 1994, *ApJ*, 436, L161  
 Chayer P., Fontaine G., Wesemael F., 1995b, *ApJS*, 99, 189  
 Cunto W., Mendoza C., Ochsenbein F., Zeippen C.J., 1993, *A&A*, 275, L5  
 Dreizler S., 1999, in *The 11<sup>th</sup> European Workshop on White Dwarfs*, ed. Jan-Erik Solheim, The ASP Conference Series, in press  
 Dreizler S., 2000, *A&A*, submitted  
 Dreizler S., Werner K., 1993, *A&A* 278, 199  
 Dreizler S., Werner K., 1996, *A&A*, 314, 217  
 Dreizler S., Wolff B., 1999, *A&A*, in press  
 Dreizler S., Heber U., 1998, *A&A*, 334, 618  
 Dupuis J., Vennes S., Bowyer S., Pradhan A.K., Thejll P., 1995, *ApJ*, 455, 574  
 Finley D.F., Koester D., Basri G., 1997, *ApJ* 488, 375  
 Holberg J.B., Barstow M.A., Bruhweiler F.C., Hubeny I., Green E.M., 1999, *ApJ*, 517, 850  
 Holberg J.B., Barstow M.A., Sion E.M., 1998, *ApJ Suppl*, 119, 207  
 Holberg J.B., Barstow M.A., Sion E.M., 1999, *ASP Conference Series Vol 169, 11th European Workshop on White Dwarfs*, eds. J-E Solheim & E. Meistas, (San Francisco: ASP), p.485  
 Holberg J.B., et al., 1993, *ApJ*, 416, 806  
 Holberg J.B., Hubeny I., Barstow M.A., Lanz T., Sion E.M., Tweedy R.W., 1994, *ApJ*, 425, L105  
 Hubeny I., 1988, *Comp.Phys.Comm.*, 52, 103  
 Hubeny I., Lanz T., 1992, *A&A*, 262, 501  
 Hubeny I., Lanz T., 1995, *ApJ*, 439, 875  
 Kidder K.M., 1991, PhD Thesis, University of Arizona  
 Kurucz R.L., 1988, in *IAU Trans.*, ed. M. McNally, VolXXB, Kluwer, Dordrecht, 168  
 Lanz T., Barstow M.A., Hubeny I., Holberg J.B., 1996, *ApJ*, 473, 1089  
 Napiwotzki R., 1992, in *The Atmospheres of Early Type Stars*, eds. U. Heber & C.S. Jeffery, *Lecture Notes in Physics* 401, Springer-Verlag (Heidelberg), 310  
 Napiwotzki R., Rauch T., 1994, *A&A*, 285, 603  
 Press W.H., Teulosky S.A., Vetterling W.T., Flannery B.P., 1992, *Numerical Recipes* (2nd edition), p687ff, Cambridge  
 Shafer R.A., Haberl F., Arnaud K.A., Tennant A.F., 1991, *ESA TM-09*  
 Sion E.M., Holberg J.B., Barstow M.A., Scheible M.P., 1997, *AJ*, 113, 364  
 Vennes S., Dupuis J., Chayer P., Polomski E.F., Dixon W.V.D., Hurwitz M., *ApJ*, 500, L41  
 Werner K., 1986, *A&A* 161, 177  
 Werner K., Dreizler S., 1994, *A&A*, 286, L31  
 Werner K., Dreizler S. 1999, in *The Journal of Computational and Applied Mathematics*, eds. H. Riffert & K. Werner, Elsevier Press, Amsterdam, in press.  
 Werner K., Dreizler S., Wolff B. 1995, *A&A* 298, 567  
 Wesemael F., Green R.F., Liebert J., 1985, *ApJS*, 58, 379  
 Wolff B., Koester D., Jordan S., Haas S., 1998, *A&A*, 329, 1045